



# Low-frequency current noise and resistance fluctuations in multiwalled carbon nanotubes

R. Tarkiainen\*, L. Roschier, M. Ahlskog, M. Paalanen, P. Hakonen

*Low Temperature Laboratory, Helsinki University of Technology, FIN-02015 HUT, Finland*

Received 20 January 2005; accepted 24 January 2005

Available online 26 April 2005

## Abstract

We have measured low-frequency current noise of arc-discharge-grown multiwalled carbon nanotube samples. At room temperature, the noise spectrum displays a regular  $\text{const}/f^\beta$  dependence with  $\beta \sim 1$  and a noise current close to  $10 \text{ pA}/\sqrt{\text{Hz}}$  at  $100 \text{ nA}$  and  $100 \text{ Hz}$ . The noise power decreases by 1–2 orders of magnitude when cooling down to  $4.2 \text{ K}$ . Due to the two-probe measurement, contacts are a likely source of the noise. At  $4.2 \text{ K}$  and below, we observe noise spectra consisting of a few Lorentzian line shapes, each of which arises due to fluctuations between two current values. The switching rates depend on the bias and they are asymmetric with respect to the direction of the current.

© 2005 Elsevier B.V. All rights reserved.

PACS: 72.70.+m; 73.63.Fg

Keywords: Carbon nanotubes;  $1/f$  noise

## 1. Introduction

Ordinary electrical components display low-frequency noise with a  $1/f^\beta$  spectrum [1,2], and several experiments have shown that carbon nanotubes [3,4] make no exception [5–12]. Collins et al. measured  $1/f$  noise of several samples of single-walled nanotubes (SWNTs), and found them to be so noisy that their use as electronic components is compromised [5], at least at room

temperature. On the contrary, extremely good noise properties have been achieved for single electron transistors made out of multiwalled carbon nanotubes (MWNTs). Roschier et al. [6] measured the charge sensitivity for a free-standing MWNT SET at sub-Kelvin temperatures and found noise properties equalling conventional, metallic SET devices. Hence,  $1/f$  noise does not present any problems when operating nanotube SETs at small currents where the squared current dependence of the noise power is still irrelevant. Undoubtedly, when optimizing nanotube devices with respect to temperature and

\*Corresponding author.

E-mail address: [reeta.tarkiainen@hut.fi](mailto:reeta.tarkiainen@hut.fi) (R. Tarkiainen).

current, a fundamental understanding of  $1/f$  noise would be instrumental.

In this paper we report measurements of low-frequency current noise in five arc-discharge-grown MWNTs. The power spectra of noise have been recorded at temperatures of 295, 77, and around 4.2 K, and we find that the noise decreases moderately with temperature. At liquid helium temperatures, instead of the usual  $1/f$  type of spectra, we observe Lorentzian line shapes resulting from one or a few systems undergoing two-level fluctuations. We analyze these spectra in terms of resistance fluctuations  $\Delta R$  and obtain  $\Delta R \simeq 1 \text{ k}\Omega$ , most likely caused by changes in the contact resistance.

## 2. Samples and measurements

Our samples were made of MWNTs, produced using the arc-discharge method. Single nanotubes, approximately 20 nm in diameter and  $1 \mu\text{m}$  in length, were positioned across a gap between two wide, prepatterned gold electrodes using an atomic force microscope (AFM) according to the scheme described in Ref. [13]. In most cases the nanotube bridging the gap remains straight and does not touch the silicon substrate. Usually, the nanotubes deposited on top of the electrodes have initially very bad contacts, showing resistances up to several megaohms. To improve electrical contact, the samples were heat treated in vacuum at  $700^\circ\text{C}$  for approximately 30 s [14]. The geometry of each sample is given in Table 1.

Transport measurements on some of these samples have been reported earlier in Ref. [15]. All of our samples show more or less pronounced Coulomb blockade below 4.2 K, indicating that the contacts are not ohmic. The analysis in Ref. [15] suggests that at high bias voltages the resistivity of the nanotubes is less significant than their high-frequency impedance  $Z = \sqrt{l_{\text{kin}}/c} = 1.3\text{--}7.7 \text{ k}\Omega$ , where  $c$  is the capacitance per unit length and the kinetic inductance  $l_{\text{kin}} \approx 1 \text{ nH}/\mu\text{m}$ . Nevertheless, some small resistivity exists because typically plasmon resonances are not observed, but we estimate that it is not larger than  $10 \text{ k}\Omega/\mu\text{m}$ . Therefore the MWNT only contributes a few

Table 1  
Dimensions of our samples

Sample	$D$ (nm)	$L_{\text{total}}$ ( $\mu\text{m}$ )	$L_{C_1}/L_{C_2}$ ( $\mu\text{m}$ )	Free-standing?
1	15	1.3	0.4/0.4	Yes
2	13	0.8	0.06/0.2	No
3	32	1.1	0.2/0.4	Yes
4	15	1.4	0.4/0.4	?
5	20	2.6	0.8/1.2	Yes

$D$  is the diameter and  $L_{\text{total}}$  denotes the length of the nanotube. The length of the contact between the tube and the electrode is given for each contact ( $L_{C_1}/L_{C_2}$ ). The length of the section between the electrodes is  $L_{\text{free}} = L_{\text{total}} - L_{C_1} - L_{C_2}$ . The last column describes the geometry: whether the tube is free-standing or not. Sample 4 was not manipulated using AFM as it was bridging the electrodes already after deposition, and hence it is not clear if it is completely free-standing or not.

kiloohms to the total resistance, and we estimate the contact resistances to be  $4\text{--}200 \text{ k}\Omega/\text{contact}$ . With the possible exception of sample 5, the measured two-probe resistance is dominated by the contacts.

To measure current and its fluctuations, we applied voltage bias at one end of the sample while the other end was monitored by a current preamplifier, either SR570 (Stanford Research) or DL1211 (DL-Instruments). Noise was recorded using an HP3561A dynamic signal analyzer. In our measurements, the frequency  $f$  was typically in the range from 1 to 500 Hz, limited by the capacitance of the wiring and the long time stability of the system. Most of the data were obtained at three stable temperatures: room temperature, 77 and 4.2 K, with a few additional measurements at lower temperatures.

## 3. Regular $1/f$ noise at 295 and 77 K

At room temperature and at 77 K the noise power had  $1/f^\beta$  character as expected. Fig. 1 shows a few examples of the spectra measured on sample 1. All our data can be accounted for by the formula

$$S_I = \frac{AI^\alpha}{f^\beta}. \quad (1)$$

The values of the exponents  $\alpha$  and  $\beta$  are given in Table 2 for each sample. These values were extracted from the data by two consecutive fitting procedures. First, the function  $S_I^{(i)}(f) = B_i/f^{\beta_i}$  was fitted to each individual  $S_I^{(i)}$  vs.  $f$  spectra, measured at different current values  $I_i$ . The value for  $\beta$  was then fixed using the average  $\beta = (1/N)\sum \beta_i$ . Subsequently, the current exponent was obtained by fitting  $S_I^{(i)}(f_0) = B_i/f_0^{\beta_i}$  vs.  $I_i$  at a fixed frequency, e.g.  $f_0 = 100$  Hz, by the function  $S_I(I, f_0) = AI^\alpha/f_0^\beta$ . For all our samples,  $\beta$  falls quite close to one, with the average value of  $\beta = 1.08$  well in line with the previous studies [5,10]. At low currents ( $I < 10$  nA), which were excluded

from the fit, crossover to thermal noise was visible at high frequencies, and the noise level was found to be consistent with the measured resistance.

The current exponent  $\alpha = 2$  is expected for pure resistance fluctuations in ohmic conductors. The measured values of  $\alpha$  in Table 2 are scattered around two, and the deviations are mainly within the error bars. The deviation is the largest for sample 2 at 77 K, where we find  $\alpha = 1.54$ , which is way beyond the scatter in the data, so a real deviation is observed. While three of the samples (1, 4, and 5) show no deviation from Ohm's law at 77 or 295 K in the employed current range ( $I \lesssim 2$   $\mu$ A), in samples 2 and 3 linear  $I$ - $V$  characteristics extend only up to 100 and 300 nA (1 and 10 nA) at 295 K (77 K), respectively. Thus, the  $\alpha \neq 2$  behavior is associated with nonlinear characteristics, and the fact that  $\alpha < 2$  suggests that  $S_I/I^2$  scales proportionally to the resistance. Assuming noncoherent noise sources, a minor effect can also arise from the relative change of the voltage drop, which is not evenly distributed over the sample. Similar behavior, with  $\alpha$  from 1 to 1.5, has been observed in CVD-grown MWNTs at very large currents [12], while in Ref. [10] a nonlinear sample, the junction between two nanotubes, was studied and an opposing result  $\alpha > 2$  was found.

The level of noise is characterized in Table 2 at  $f = 100$  Hz and  $I = 100$  nA. Except for sample 2, all the samples fall quite close to each other, with the noise power of 8–200  $\text{pA}^2/\text{Hz}$  (6–20  $\text{pA}^2/\text{Hz}$ ) at  $T = 295$  K ( $T = 77$  K). The decrease in noise level when going from room temperature to 77 K is illustrated in Fig. 1 (sample 1). At 4.2 K, we find

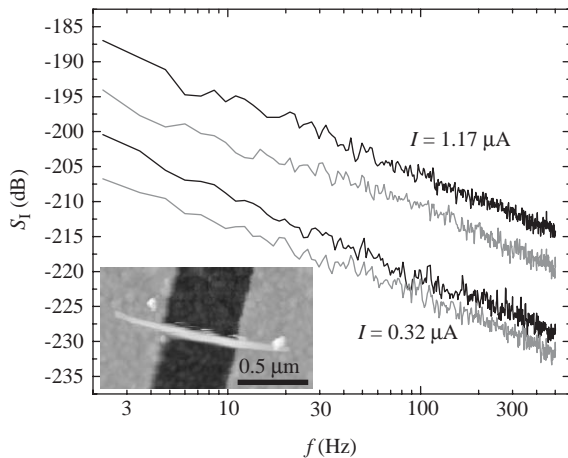


Fig. 1. Current noise power spectra of sample 1 at room temperature (black) and 77 K (gray). The change with temperature equals 3 dB at  $I = 0.32$   $\mu$ A and 5 dB at  $I = 1.17$   $\mu$ A on average. Inset: an AFM picture of sample 1.

Table 2

Noise current and frequency exponents  $\alpha$  and  $\beta$ , and inter-/extrapolated noise power at  $f_0 = 100$  Hz and  $I = 100$  nA

Sample	$R_{295\text{K}}$ (k $\Omega$ )	$S_I$ (295 K) ( $\text{pA}^2/\text{Hz}$ )	$\beta_{295\text{K}}$	$\alpha_{295\text{K}}$	$R_{77\text{K}}$ (k $\Omega$ )	$S_I$ (77 K) ( $\text{pA}^2/\text{Hz}$ )	$\beta_{77\text{K}}$	$\alpha_{77\text{K}}$	$R_{4\text{K}}$ (k $\Omega$ )	$S_I$ (4 K) ( $\text{pA}^2/\text{Hz}$ )
1	33	8	1.07	2.28	53	6	1.03	2.00	55	1
2	390	$40 \times 10^3$	1.09	1.75	2450	$2 \times 10^3$	1.09	1.54	620/910 <sup>a</sup>	300
3	133	200	1.15	2.04	801	8	1.16	2.12	275	1
4	—	—	—	—	70	20	0.94	1.87	106	1
5	13	90	1.07	1.93	26	20	— <sup>b</sup>	1.79	49	4

The linear resistance is given for 295 and 77 K, while the 4 K value is the differential resistance at 100 nA.

<sup>a</sup>The differential resistance is asymmetric with respect to the current direction.

<sup>b</sup>The experimental value was not determined.  $\beta = 1$  was assumed for extrapolation.

that the  $1/f$  structure of Eq. (1) cannot account for the data anymore. Instead, the measured noise spectra are composed of a sum of a few Lorentzian line shapes:

$$S_I = I^2 \sum_i \frac{S_L^{(i)} \tau_i}{1 + 4\pi^2 \tau_i^2 f^2}, \quad (2)$$

where each Lorentzian is characterized by a lifetime  $\tau_i$  and an amplitude  $S_L^{(i)}$ . These Lorentzians are found to depend on the bias voltage, which leads to irregular and nonmonotonic current dependence of the noise. The irregular behavior is illustrated in Fig. 2 for sample 1. Disregarding the irregular details, there is a reduction, on the order of 10 dB, in the average  $1/f$  noise when temperature decreases from 295 K down to 4.2 K. In Table 2, the magnitude of the noise power at 4.2 K is estimated by an approximate fitting procedure at  $f = 100$  Hz and  $I = 100$  nA, or picked from a representative spectrum, if no fitting procedure was feasible. According to the generic  $1/f$  model, the individual fluctuations are thermally activated, and freeze out, as the temperature is lowered. Eventually, so

few sources are left that they show up as individual Lorentzians. The noise scales as  $S_I \propto k_B T D(\tilde{E})$ , where  $D(E)$  is the distribution of the activation energies and  $\tilde{E} = -k_B T \ln(2\pi f \tau_0)$ , where  $\tau_0^{-1}$  is the attempt frequency [16]. Assuming weakly energy-dependent  $D(E)$ , our samples fall quite close to this model. The temperature dependence of the noise in our samples is more moderate than measured previously in SWNTs [8].

The variation in noise level from sample to sample is not clearly correlated with any measurable parameters such as sample resistance. Since  $1/f$  noise in tunnel junctions is inversely proportional to the junction area, the anomalously high noise level in sample 2 could originate from the very short contact at one end of the nanotube. Among the other samples there is no connection between contact length and noise level. However, it is not possible to know accurately how a large part of the overlap between the nanotube and the electrode is actually conducting. All MWNTs except sample 4 were manipulated using an AFM, but the noise level of sample 4 is well in line with the others, and thus no connection between manipulation and the noise levels can be proven.

To facilitate comparison between earlier work, we use a value  $A = S_I f / I^2$ , which is not strictly a constant but a weak function of  $I$  and  $f$ . Anyway, at room temperature we obtain  $A = 8 \times 10^{-8} - 4 \times 10^{-4}$  in our samples. This is comparable to  $A = 3 \times 10^{-7}$  reported for a MWNT [10]. For individual SWNTs, Collins et al. found  $A \approx 10^{-5}$  [5], and Postma et al. found  $A = 3 \times 10^{-5}$  [8], which are towards the high end of our range. Very low  $1/f$  noise,  $A \approx 10^{-13}$ , was recorded for a thick rope of SWNTs [9]. At a very large current,  $I = 0.1$  mA,  $A \approx 10^{-10}$  has been observed for a MWNT, but that value is not likely to extrapolate well down to low currents [12].

Based on their measurement on SWNTs, Collins et al. [5] present an empirical model according to which the noise level is directly proportional to the sample resistance. The model was confirmed by Snow et al. [11] for 2D SWNT mats, and in addition direct dependence on size was found. We find that the noise levels in our samples are in accordance with this phenomenological model.

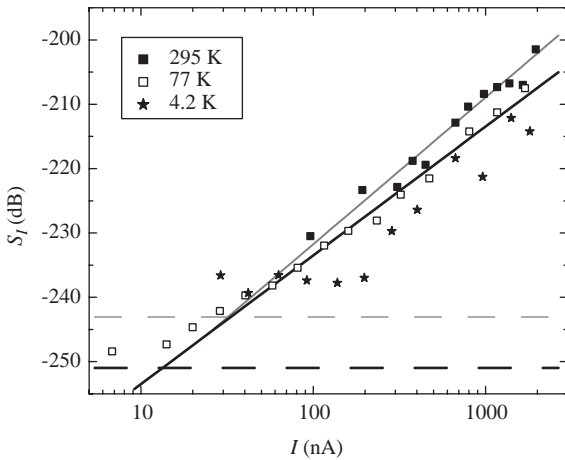


Fig. 2. Current noise spectral density of sample 1 at three different temperatures ( $f = 121$  Hz). The solid lines were calculated using the parameters given in Table 2. The horizontal lines indicate the thermal noise level at 295 K (thin dashed line) and at 77 K (thick dashed line). Towards low currents ( $I < 100$  nA), the 4.2 K noise levels off, suggesting that in this regime background charge fluctuations, which induce modulation of the current due to the Coulomb charging effects, become important. A similar effect was seen in sample 4.

Values calculated using Eq. (1) of Ref. [5] reproduce our measured noise levels (Table 2) within a factor of 0.1–3, except for sample 2 which, as noted above, has a considerably higher noise. Our results are consistent with this model in the sense that, in general, MWNT samples have lower resistances than SWNT samples, and therefore lower noise levels, as observed in our measurements, are indeed expected. However, our samples as such do not indicate any clear connection between resistance and noise level.

A linear increase of noise level with resistance can be understood if the samples consist of several parallel conduction channels [5]. In this case the resistance is inversely proportional to the number of channels  $M$ , while  $1/f$  noise, according to Hooge's empirical formula [17], scales as  $\propto 1/N$ , where  $N$ , the number of free charge carriers, is proportional to system size. As  $N \propto M$ , it follows that  $S_I \propto R$ . This reasoning applies to a selection of samples, in which the conductivity is determined by the number of parallel conduction paths. However, there is no obvious reason why this scaling should hold among individual nanotubes. On the contrary, one would expect the resistance to be directly proportional to sample length  $L$ , as well as  $N \propto L$ , which would give  $S_I \propto 1/R$ . Such dependence is not observed.

In our samples, most of the voltage drop actually occurs at the contacts, obscuring any correlation between the resistance and the system size. The contacts are a likely source of noise, because, assuming incoherent noise sources, as the most resistive part of the system, they weaken the coupling of noise from other parts of the sample to the external circuit.

In bulk samples,  $1/f$  noise arises from resistance fluctuations, which may be described as fluctuations in either carrier number or mobility [2]. The microscopic origin of the fluctuations is typically charge traps. In MWNTs the current is mainly carried by the outermost layer at low temperatures, and even though a perfect nanotube has no intrinsic surface states owing to its closed structure, TEM investigations have revealed that nanotube surfaces are often contaminated by amorphous carbon and nanoparticles. Therefore, it seems plausible that there exists localized states,

which may act as traps. In addition to “on-tube”  $1/f$  noise, the contacts are a probable source of resistance fluctuations, because there are surface states at least on the gold electrodes. Other possible trap sites are lattice defects, the inner layers in MWNTs, or localized end states.

Altogether, we find the  $1/f$  noise in MWNTs to be more manageable than in SWNTs due to size scaling and/or smaller resistance. At low temperatures, the noise power drops, and this makes nanotube devices more practicable under these special circumstances.

#### 4. Two-level fluctuators at low temperatures

At 4.2 K and below, the power spectra can be described by using a sum of a few terms of the form  $S_I/I^2 = S_L\tau/(1 + 4\pi^2\tau^2f^2)$ . The noise signal, which gives rise to the Lorentzian line shapes, consists of switching between two current states, with a typical lifetime of each state given by  $\tau$ . Such fluctuations, called random telegraph signals, were also visible in the time traces measured on our MWNT samples, when the lifetime was long enough for observation by our setup. Random telegraph noise (RTN) is well known from many systems, e.g. tunnel junctions [18], MOSFET channels [19], and SETs [20]. In SETs, RTN signals are typically attributed to background charge fluctuations [6,7]. In nanotube SETs, the background charge fluctuations were sufficient to account for only part of the noise, and an additional current-dependent contribution was clearly visible [7]. The charge fluctuations are not important at high voltages  $V \gg e/4C_T$  where the single-electron charging effects have negligible effect on the conduction. In our samples, we have estimated that  $C_T \simeq 30$  aF [15], and thus the contribution of background charge fluctuations can be neglected at bias voltages above a few tens of millivolts. However, in our nanotubes the TLF behavior prevails over the entire current range studied ( $|I| < 3 \mu\text{A}$ ).

The details of the measured power spectra at 4.2 K depend strongly on sample biasing and they are different for each individual sample. In our frequency band of 1–500 Hz, we were able to resolve only 1–2 Lorentzians simultaneously,

accompanied by a small, overall  $1/f$  background. The two parameters characterizing an individual fluctuator, the magnitude  $S_L$  and the lifetime  $\tau$ , were both found to depend on the bias current. The situation is illustrated in Fig. 3 for sample 4. In this case, the corner frequency of the spectrum shifts towards higher frequencies as the average current is increased. Such behavior totally modifies the shape of the  $S_I$  vs.  $I$  curves: the noise level, measured at constant frequency, does not follow a simple power law any more. A broad peak appears around the current value, where the current-dependent corner frequency  $1/2\pi\tau(I)$  equals the fixed measurement frequency. In this sample, a similar peak can be detected if the direction of the bias is reversed, but at a slightly different position: the peaks occur at  $-1.1$  and  $0.7\mu\text{A}$ . One can also easily discern the broad maxima in the noise due to these two-level fluctuations in the differential resistance (Fig. 4), measured using lock-in techniques at a few tens of hertz. The differential resistance shows a typical Coulomb blockade peak at zero bias, indicating that tunnel junctions are formed at the contacts, and some additional asymmetric structure.

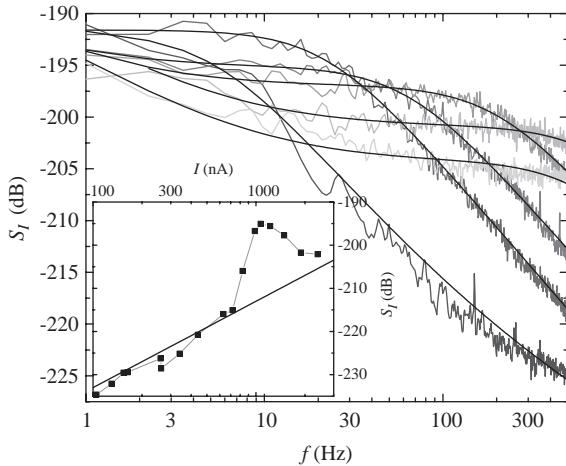


Fig. 3. A few spectra that show TLF type of behavior (sample 4). The average currents corresponding to the spectra are 0.82, 1.07, 1.22, 2.39, 1.49, and  $1.89\mu\text{A}$ , respectively, from bottom to top, at 500 Hz. While bias voltage is increased, the corner of the spectrum moves to right ( $\tau$  decreases). For the fitted curves, see the text. The inset shows the corresponding noise ( $f = 25\text{ Hz}$ ) vs. average current plot, which shows a broad peak on top of the  $I^2$  background.

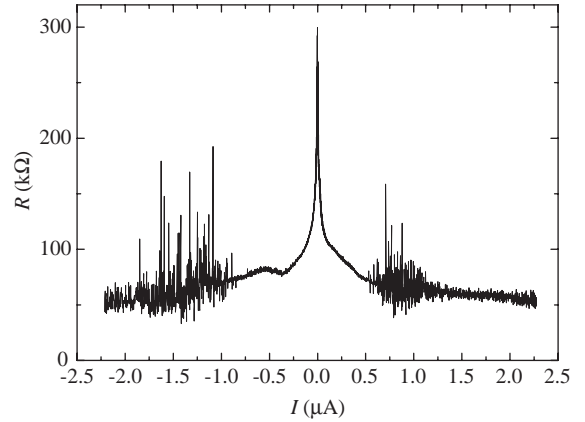


Fig. 4. Differential resistance of sample 4, measured at  $T = 1.5\text{ K}$  using small AC excitation at low frequency (on the order of 30 Hz). Due to sudden jumps of the current, caused by the active TLFs, the lock-in amplifier tends to lose its phase, which is seen as high spikes in the trace.

The fitted curves in Fig. 3 are obtained by using Eq. (2), with the aid of  $1/f$  background to account for those Lorentzians whose corner frequency is outside our bandwidth. One obtains the parameters characterizing individual two-level fluctuators (TLF)  $\tau$  and  $S_L$ , which are shown in Fig. 5 as a function of the average current. In this sample, there are three dominating TLFs within 1–500 Hz, data sets labeled I, II and III in Fig. 5. The data at both bias directions are combined on a single axis, so that TLF III is actually active at opposite bias direction as I and II. For all three cases, the lifetimes decrease approximately exponentially with the magnitude of the current. This has been found to be the typical case for TLFs in tunnel junctions [21]. It is possible that fluctuations seen at opposite current directions, such as II and III, originate from the same physical TLF. A TLF located asymmetrically to the tunnel junction can have different coupling in each bias direction [22].

The peaking of  $S_L$  visible in Fig. 5b can be understood if the time constants for the two current states are not equal. Machlup has shown that the power spectrum of such a system is also a Lorentzian [23], with

$$\frac{1}{\tau_{\text{eff}}} = \frac{1}{\tau_1} + \frac{1}{\tau_2}, \quad (3)$$

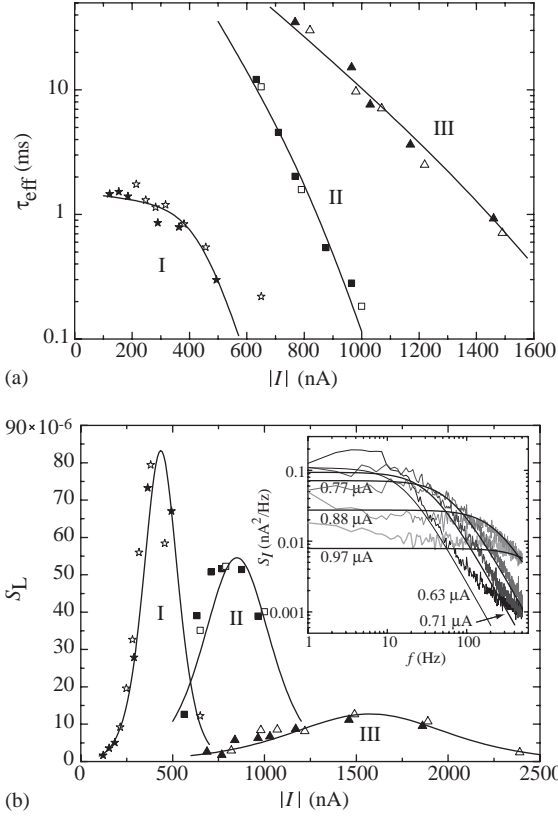


Fig. 5. (a) Effective time constants extracted from power spectra (see Fig. 3) as a function of average current and (b) the corresponding TLF magnitudes  $S_L$  for sample 4. The data sets labeled I, II and III correspond to the three dominating TLFs seen in the frequency range 1–500 Hz. The fluctuators I and II occur with the same polarity of bias voltage, while III is observed at opposite bias. Points measured at 4.2 K (filled symbols) and 1.5 K (open symbols) are displayed. The solid lines are obtained by simultaneously fitting Eq. (3) to the time constants in (a) and Eq. (4) to magnitudes in (b). In the inset, a few of the original spectra are reproduced by the five-parameter model of one dominant fluctuator (data set II).

where  $\tau_1$  and  $\tau_2$  are the time constants of the two current states, and

$$S_L = \frac{S_0 \tau_{\text{eff}}}{\tau_1 + \tau_2}, \quad (4)$$

where  $S_0 = 4(\Delta I/I)^2$  and  $\Delta I$  is the change in current between the two states. The solid lines in Figs. 5a and b are obtained using a phenomenological model, following the procedure done for tunnel junctions in Ref. [18], where each time

constant is assumed to depend on bias exponentially:  $\tau_i = \tau_0^{(i)} \exp(-I/I_0^{(i)})$ ,  $i = 1, 2$ . A simultaneous fit of Eqs. (3) and (4) with five parameters  $S_0$ ,  $\tau_0^{(1)}$ ,  $\tau_0^{(2)}$ ,  $I_0^{(1)}$ , and  $I_0^{(2)}$  yields the solid curves. If the number of fitting parameters is reduced to four by, for example, assuming one rate to be constant, it is no longer possible to obtain a satisfactory fit.

Assuming resistance to be the fluctuating quantity,  $\Delta I/I = \Delta R/R$ , from the magnitude  $S_0 = 4(\Delta R/R)^2$  we obtain the following values for  $\Delta R$ : 910, 660, and 270  $\Omega$  for the three TLFs I, II, and III, respectively. Despite the striking analogy with defects in tunnel junctions, is it possible that the noise originated from the tube itself? The resistance change is quite large compared with our estimate of tube resistance of 5 k $\Omega$ . If  $\Delta R$  originated from universal conductance fluctuations (UCF), we would expect it to vary with temperature, as the ratio of the dephasing length to the sample length  $L_\phi/L$  is still expected to grow between 4 and 1 K [25]. However, the TLF parameters do not show much change going from 1.5 to 4.2 K. The measured  $\Delta R$  corresponds roughly to a UCF amplitude of  $e^2/h$ , suggesting that the sample is nearly phase coherent. In a nonequilibrium situation, such as our experiment, inelastic scattering has been observed to destroy the quantum interference [26], and hence, under the circumstances, the fluctuation amplitude of  $\sim 1$  k $\Omega$  seems too large for UCF. If the resistance change originates from one of the contacts, e.g. from a charge trap altering the tunneling barrier transmission, a change of the above magnitude can easily occur.

One has to keep in mind, however, that the lack of temperature dependence can also be an indication of electron heating: at the strongly nonequilibrium situation, the tunneling electrons have energies much higher than 4.2 K, and due to the ‘semi-ballistic’ nature of transport, they are not likely to thermalize before leaving the nanotube. This results in a nonequilibrium distribution with electron energies much above the lattice temperature. It is also possible that the current directly causes the noise via some mechanism, and not only scales the existing fluctuations.

The lack of temperature dependence, if not a heating effect, points to the regime of quantum

tunneling, which occurs when the temperature of a two-level system is below the thermally activated region. Such behavior has been observed previously in tunnel junctions [24], where the fluctuators were identified as electron traps in the amorphous junction oxide. Using WKB-approximation, the lifetime is given by

$$\begin{aligned} \frac{1}{\tau} &= \frac{1}{\tau_0} \exp\left(-\frac{2}{\hbar} d \sqrt{2mE_b} C(1 - \gamma V)\right) \\ &= \frac{1}{\tau_0} \exp(-C'(1 - \gamma R_{\text{eff}} I)), \end{aligned} \quad (5)$$

where  $C$  and  $\gamma$  are numerical parameters depending on the shape of the potential barrier,  $E_b$  and  $d$  are the barrier height and width, respectively, and  $\tau_0^{-1}$  denotes the attempt frequency. The voltage over the trap couples to the current via some effective resistance:  $V = R_{\text{eff}} I$  and  $C' = 2d\sqrt{2mE_b}C/\hbar$ . This model readily yields the current dependence utilized in fitting the data.

As illustrated above by sample 4, the observed noise behavior is highly asymmetric with respect to the bias. This applies to all of our samples. This is in accordance with the view that the contacts act as sources of the resistance fluctuations. If the TLF is located asymmetrically with respect to the junction, its coupling to the current will depend on the direction of the bias [22]. The structure of our tunnel junctions is not well understood, but there is no oxide layer, where the TLF could reside. Therefore, the TLF is either on one side of the interface or on the other, i.e. in the electrode or in the nanotube, and asymmetry appears as a natural consequence.

Similar current-dependent fluctuations were observed also on samples 1, 2 and 3. However, detailed analysis was not achieved for these samples. When the spectrum consists of a superposition of several Lorentzians it becomes very difficult to observe their evolution separately. Also, the TLF configuration may be unstable and change irreversibly, when voltage and temperature are being changed. This was the case especially in sample 3. In sample 5 we did not observe any current-dependent TLFs. There was one dominating TLF, but its corner frequency appeared to be practically constant,  $f \approx 60$  Hz.

This can be understood if the TLF is situated so that there is no electric field over it, and therefore it does not couple to the transport bias.

## 5. Conclusions

We have measured current noise in arc-discharge-grown multiwalled carbon nanotubes. In general, we find that the level of low-frequency excess noise decreases by a factor of 10–100 when temperature is lowered from 300 to 4 K. At 4.2 K, single fluctuators play a significant role in the noise behavior of carbon nanotubes. A model with exponentially current-dependent time constants was utilized to explain the measured current noise spectra, reminiscent of findings in tunnel junctions. In addition, we find that the noise characteristics are different for opposite bias directions. The metal–nanotube contacts are a likely source for these fluctuations. However, due to the large number of factors that may contribute to the fluctuations, the exact origin of the noise cannot be pinpointed in our experiments.

## Acknowledgements

We thank Catherine Journet and Patrick Bernier from the University of Montpellier for supplying us with the high-quality, arc-discharge-grown nanotubes. Useful discussions with Edouard Sonin are gratefully acknowledged. This work was supported by the Academy of Finland and TEKES.

## References

- [1] M.J. Buckingham, *Noise in Electronic Devices and Systems*, Wiley, New York, 1983.
- [2] A. van der Ziel, *Noise in Solid State Devices and Circuits*, Wiley, New York, 1986.
- [3] S. Iijima, *Nature* 354 (1991) 56.
- [4] For reviews, see e.g., Special issue on nanotubes in *Physics World*, June 2000, p. 29.
- [5] P.G. Collins, M.S. Fuhrer, A. Zettl, *Appl. Phys. Lett.* 76 (2000) 894.
- [6] L. Roschier, R. Tarkiainen, M. Ahlskog, M. Paalanen, P. Hakonen, *Appl. Phys. Lett.* 78 (2001) 3295.



- [7] M. Ahlskog, R. Tarkiainen, L. Roschier, P. Hakonen, *Appl. Phys. Lett.* 77 (2000) 4037.
- [8] H.W.Ch. Postma, T.F. Teepen, Z. Yao, C. Dekker, in: T. Martin, G. Montambaux, J. Trân Thanh Vân (Eds.), *Electronic correlations: from meso- to nano-physics*, Proceedings of the XXXVIth Rencontres de Moriond, EPD Sciences, France, 2001, p. 433.
- [9] P.-E. Roche, M. Kociak, S. Guéron, A. Kasumov, B. Reulet, H. Bouchiat, *Eur. Phys. J. B* 28 (2002) 217.
- [10] H. Ouacha, M. Willander, H.Y. Yu, Y.W. Park, M.S. Kabir, S.H.M. Persson, L.B. Kish, A. Ouacha, *Appl. Phys. Lett.* 80 (2002) 1055.
- [11] E.S. Snow, J.P. Novak, M.D. Lay, F.K. Perkins, *Appl. Phys. Lett.* 85 (2004) 4172.
- [12] R. Vajtai, B.Q. Wei, Z.J. Zhang, Y. Jung, G. Ramanath, P.M. Ajayan, *Smart Mater. Struct.* 11 (2002) 691.
- [13] M. Martin, L. Roschier, P. Hakonen, Ü. Parts, M. Paalanen, B. Schleicher, E.I. Kauppinen, *Appl. Phys. Lett.* 73 (1998) 1505.
- [14] J. Lee, C. Park, J. Kim, J. Kim, J. Park, K. Yoo, *J. Phys. D* 33 (2000) 1953.
- [15] R. Tarkiainen, M. Ahlskog, J. Penttilä, L. Roschier, P. Hakonen, M. Paalanen, E. Sonin, *Phys. Rev. B* 64 (2001) 195412-1; samples 1 and 4 here correspond to samples T1 and T3.
- [16] P. Dutta, P. Dimon, P.M. Horn, *Phys. Rev. Lett.* 43 (1979) 646.
- [17] F.N. Hooge, *Phys. Lett. A* 29 (1969) 139; F.N. Hooge, *IEEE Trans. Electron. Devices* 41 (1994) 1926.
- [18] C.T. Rogers, R.A. Buhrman, *Phys. Rev. Lett.* 53 (1984) 1272.
- [19] K.S. Ralls, W.J. Skocpol, L.D. Jackel, R.E. Howard, L.A. Fetter, R.W. Epworth, D.M. Tennant, *Phys. Rev. Lett.* 52 (1984) 228.
- [20] S.M. Verbrugh, M.L. Benhamada, E.H. Visscher, J.E. Mooij, *J. Appl. Phys.* 78 (1995) 2830.
- [21] C.T. Rogers, Ph.D. Thesis, Cornell University, 1987.
- [22] X. Jiang, M.A. Dubson, J.C. Garland, *Phys. Rev. B* 42 (1990) 5427.
- [23] S. Machlup, *J. Appl. Phys.* 25 (1954) 341.
- [24] C.T. Rogers, R.A. Buhrman, *Phys. Rev. Lett.* 55 (1985) 859.
- [25] C. Schönenberger, A. Bachtold, C. Strunk, J.-P. Salvetat, L. Forró, *Appl. Phys. A* 69 (1999) 283.
- [26] C. Terrier, D. Babić, C. Strunk, T. Nussbaumer, C. Schönenberger, *Europhys. Lett.* 59 (2002) 437.